

**AMM014**

## **A Time-Frequency Study on Target Response to Impact**

Paul W. Bland<sup>1\*</sup>, Petch Jearanaisilawong<sup>2</sup>, Pitiphong Atibodhi<sup>1</sup>, Banleng Sornhil<sup>1</sup>

<sup>1</sup> The Sirindhorn International Thai-German Graduate School of Engineering (TGGS),  
King Mongkut's University of Technology North Bangkok (KMUTNB), 10800, Thailand.  
<sup>2</sup> Department of Mechanical & Aerospace Engineering (MAE), KMUTNB, 10800, Thailand.

\* Corresponding Author: Tel: +66 (0) 2555 2926, Fax: +66 (0) 2555 2937,  
E-mail: pwbland72@gmail.com

### **Abstract**

The trend towards lighter automotive structures requires improved or optimized impact energy absorption and damage limitation strategies, driving the need for a better understanding of the smaller time and space scale impact mechanics. This includes the fast changing frequency content of the structure during and immediately after impact contact. A free flying projectile impacting onto a laboratory scale target was studied by experiment and simulation. The most important results presented here, arose from an off centreline axis impact condition, to excite bending and torsion modes. The work included Hammer Impact (HI) testing for modal parameter extraction as an input to a Finite Element model (FE) of target response to Projectile Impact (PI) tests. The PI tests had exactly the same mechanical conditions as for the HI set-up, and instrumented with target mounted accelerometers and a High Speed Camera (HSC). HSC frame images were analysed visually and by image processing using an edge detection method. Both experimental and simulation data sets were processed using Short Time Fourier Transform (STFT), to obtain Time-Frequency (T-F) plots, all considering bending and torsion modes. HI results confirmed a validated linear FE model of the target. STFT analysis of experimental data shows that the frequency content changes with time, and the HSC edge detection results show the 3rd torsion mode appear-disappear-reappear, which is not captured by the FE model.

**Keywords:** Impact, Time-Frequency, Nonlinear.

### **1. Introduction**

In the general case, all free flying projectile-target impact will develop a transient vibration response. Impact can be classified using temporal and/or frequency responses. Durations of an impact can last from milliseconds for low velocity impact, such as a free falling of an object, to nanoseconds for high velocity impact in ballistic projectiles. The faster the relative impact velocity is the smaller the duration of the impact becomes. The high velocity impact leads to a short duration of the wave pulses that are measured using standard sensors such as accelerometers and acoustic emission. Time-frequency analysis that relates measured temporal signal to frequency signal can be used to analyze the underlying modes of structural response. For time-variant structural systems such as those in seismic events, in contacts or with joints, the time-frequency analysis requires advanced computational techniques such as Short Time Fourier Transform (STFT) [1]. Wavelet techniques [1-4] have also been proposed to evaluate frequency response and estimate modal parameters of time-variant systems. Additional computational techniques to evaluate time-variant systems include a two-stage identification method with incomplete acceleration measurements [5], hybrid time-frequency method [6], Harmonic Balance method [7] and Hilbert-Huang transform [8].

In contrast to the variations of experimental analysis techniques, nonlinear structural dynamics cannot be effectively or efficiently simulated using finite element methods because of the simplifying

assumptions used in the simulations. For example, the choice of contact algorithms in an impact simulation can influence the simulation results [9].

In this work, the STFT method was chosen as a first step. In addition, only simple structures were considered, whereby there is no direct mechanical coupling between modes. Linear theory says that after the projectile has lost contact with the target, then whatever energy is present in the set of modes that comprise the deflection shape at that time, will only dissipate based on the damping of each mode with no gain of energy in any mode. From this point onwards, the response is free vibration decay.

Two cases of non-linear behaviour are proposed, being weak and strong behaviour. Weak non-linear behaviour adds on to the linear theory a phenomenon whereby the modal response continue to form after contact is lost, but when any given mode reaches its maximum energy content, it then dissipates that energy as in the linear case. Previous experimental work has observed such weak non-linear behaviour, under carefully controlled conditions [10]. The energy gain in the modes after contact is lost, is believed to come from the final stages of the stress wave interaction both internally and with the boundary conditions. This hypothesis is not yet proven, and is a topic of ongoing research.

The experimentally observed weak non-linear phenomenon raised the possibility of a strong non-linear phenomenon. This was proposed as being the same for the weak case, but now allowing for two or more cycles of energy to be gained-lost for one or

## AMM014

more modes after last contact. Due to there being no direct mechanical modal coupling, this would require energy to be swapped, more than once in both directions, between either the stress wave scale (micro scale) and normal mode scale (macro scale), or between the normal modes and sub-harmonic or super-harmonic modes that coupled to other normal modes, or some combination thereof. This specific definition of strong non-linear impact response after last contact is referred to in this paper as “T-F” behaviour. It would appear in the time-frequency domain as a time varying energy content in at least one modal frequency, rising and falling at least twice, and the rising (or falling) of energy content of the modes will not occur at the same time or even necessarily at the same rate.

This paper focuses on providing proof of the existence of the key phenomenon of highly transient nonlinear behaviour, characterised by T-F varying energy content of at least one mode.

### 2. Methodology

The primary objective was to create experimental test conditions that resulted in the T-F phenomenon. The secondary objective was to compare experimental observations to an FE model to check for any critical deficiencies in the model that could not match the T-F behaviour.

The overall methodology included modal testing to establish the target specimen modal properties and validation of the FE model, free flying projectile experimental impact to excite a T-F response, and simulated free flying projectile impact using the FE model to compare with experiment. Analysis included HSC visual inspection and edge detection methods. STFT analysis applied to HSC and accelerometer data, to look for time-frequency phenomena. Due to limitations of resolution, it was decided to focus on the first three bending modes (B1, B2 & B3) and the first three torsion modes (T1, T2 & T3). The main limitation was the resolution constraint of the HSC of  $10kfps$  giving a maximum frequency of  $1KHz$ .

The original work included many PI test cases, but only one case is presented in this paper for brevity and also as being sufficient on its own to show at least one instance of the key behaviour occurring. Therefore only one specimen geometry and one PI test are detailed below.

The following sub-sections give key details for the main work components.

#### 2.1 Projectile and test specimen

The projectile was a  $7g$  polyethylene hollow cylindrical cup. To save space, incomplete drawings are shown in Fig. 1, in  $mm$ . The overall cylinder shape is tapered with a lip at the rear, to provide a gas tight seal when fired in the gas gun. The projectile is actually a sabot, normally used to carry over projectile in the gun barrel and stripped before impacting the target. This function was not used in the work reported in this paper.

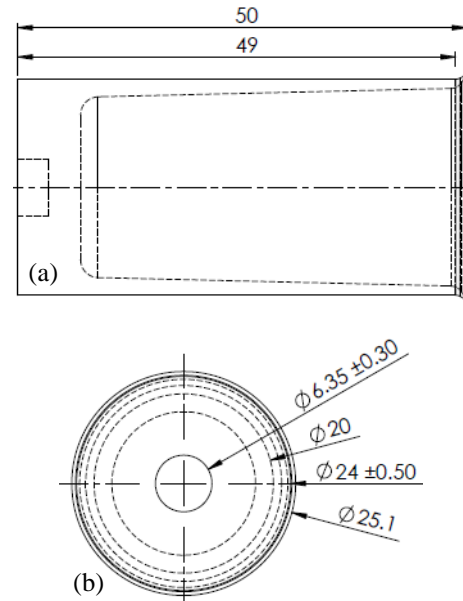


Fig.1 Projectile (a) cross section & (b) front view.

The test specimen, also referred to as “target”, was an aluminium plate,  $500 \times 50 \times 3mm$ , mounted in the vertical plane, supported only by a single pin-joint boundary condition at the top. The pin-joint condition was realised by the assembly shown in Fig. 2b and Fig. 3, comprising of a pin-joint housing that contains its own clamp plates that clamp the target over its full width and  $28mm$  of its top end, hence giving a rigid body added mass to the top end of the target but with an overall pin-joint boundary condition.

This specimen and boundary condition geometry and configuration was chosen based on previous extensive experimental impact testing experience, where pin-jointed conditions, relatively long-thin targets, relatively light projectile-target mass ratios increase the chances of observing interesting phenomena after last contact [10]. The details had to be selected from experience, and not from simulation, as there was no reason to believe any simulation could show the phenomena of interest.

Two Kistler 8794A500  $500g$  accelerometers were mounted on the rear surface, as shown in Fig. 2b, symmetric to and laterally displaced from the target centreline by  $12mm$ , and  $25mm$  from the target bottom edge, therefore being able to observe both bending and torsion modes.

#### 2.2 Projectile impact test

A custom-made Light Gas Gun was designed and built at TGGs KMUTNB, including an extensive proof of functionality and experimental impact test programme, from which this single reported test case emerged.

The critical projectile impact test of interest occurred by accident, due to the projectile having a slight misfire and not striking the target normal its surface.



Fig.2. Target (a) shown side on and mounted in the gas gun cubicle with an approaching projectile & (b) identical mounting outside of the gas gun cubicle for modal testing.

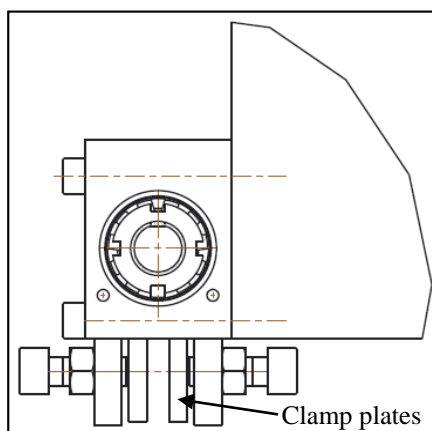


Fig.3. Side view drawing of the pin-jointed assembly.

The misfire occurred due to the very light projectile being more susceptible to asymmetrical forces and air pressures causing slight rotation. Due to the projectile's circular flat front, when impacting at a

slight angle to the normal, a small arc section of the front lip will make first contact on the target, at a location off the target centreline, and hence excite torsion modes as well as bending modes. This proved crucial to the main observations in this paper. The contact angle was confirmed by HSC video playback, to be a  $3^\circ$  rotation about the vertical axis. The centre of impact was  $156.5\text{mm}$  from the target bottom free edge as shown in Fig.4, with an impact velocity of  $17.4\text{m/s}$ .

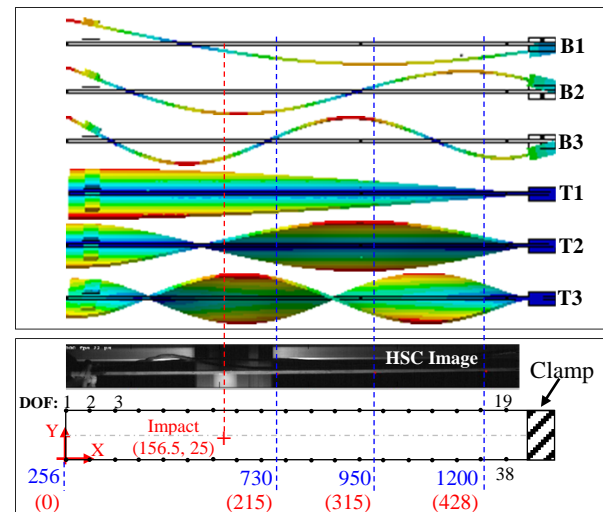


Fig. 4. Target X-direction (red) length scaled mapping of projectile impact location, validated FE mode shapes, ODS hit locations (black), and HSC viewing window pixel numbers (blue).

### 2.3 Modal test and analysis

Using exactly the same specimen and clamping arrangement, but located outside of the gas gun as shown in Fig. 2b, with the fixed accelerometer location, a 38 location roving impact hammer method was used, and analysed to give standard modal parameters as well as an Operation Deflection Shape (ODS) method to confirm the mode shapes. The hit locations were in two rows of 19, each row near the specimen long edges, starting at the bottom of the specimen and equally spaced  $25\text{mm}$  apart, covering  $450\text{mm}$  length of the specimen in the specimen co-ordinate system X-direction, as shown in Fig.4.

### 2.4 FE model

The FE model included the aluminium specimen and brass clamp plates. The accelerometers and the pin-joint assembly rotating parts were added as lumped masses in their respective locations. Validation against the modal test results included fine tuning the material properties as well as the component contact conditions between clamp plates and the specimen and also between the accelerometers and the specimen. The contact sensitivity was analysed by constraining all degrees of freedom but varying the constrained contact surface area.

### 2.5 High speed camera set-up and analysis

A HSC was set up side on to the target, triggered by infra-red beam broken by the projectile, and with a viewing window as shown in Figs.2a & 4, covering

## AMM014

most of the target length from its very bottom to 36.5mm of the specimen top edge, mapping to pixel numbers 256-1280 respectively. The viewing window size and location, combined with a frame rate of 10kfps was sufficient to view the projectile approaching, the projectile-target contact timing, and the excited modes of interest.

Visual inspection using the HSC supplied software was a first filter to identify key events and phenomena. Image processing edge detection was used for quantitative analysis, with a pixel resolution of 0.45mm. Three points along the length of the target were chosen at “pixel number” (“X-direction coordinate”) 730(215), 950(315) and 1200(428), to be able to capture the mode shapes most efficiently. The set-up could differentiate between bending and torsion due to the geometry of the field of view and decomposing motion into the modal frequency components. Rigid body swinging motion was filtered out using a Detrend function in Matlab.

### 2.6 Short Time Fourier Transform analysis

The accelerometer data and the HSC target edge displacement data are recorded in the time domain, and were processed to give time-frequency results using STFT, including varying the sampling time window. For the HSC data, this was applied to the three locations specified above, and the corresponding locations in the FE model. A simulated signal was used to form a set of criteria to judge when a mode's energy content has significantly reduced to justify stating that the mode has disappeared from the specimen response over a particular time frame. This was investigated by controlling the signal's mixed frequency content and amplitude, and by switching off one of the frequency components for a chosen short time duration, then processing that mixed signal through the STFT, and also by considering different STFT windows of 1, 3 and 5ms.

## 3. Results and Discussion

The following sections give selected results for modal testing and FE model validation, and for the single crucial projectile test, the results from HSC visual inspection and edge detection analysis, and a brief comparison of STFT analysis between experiment and simulation.

### 3.1 Modal test and validation of the FE model

The final FE model was validated with the linear HI test results for the first three bending and first six torsion modes. Good agreement confirmed qualitatively matched mode shapes with frequencies shown in Table 1. Validated mode shapes are shown in Fig. 4. The linear FE model was then used to predict, albeit with limitations, the nonlinear PI response to elucidate the uncoupled vibration response without accounting for dissipative plastic modes. The validated FE model used second order tetrahedral elements with bonding contact surface areas matching the projected screw diameter. The remaining boundary conditions

on the target and projectile replicate those in the PI test. Density, Young's modulus and Poisson's ratio for Aluminium and Brass are 2700 kg/m<sup>3</sup>, 70 GPa, 0.33 and 8490 kg/m<sup>3</sup>, 97 GPa, 0.31 respectively.

The results also confirmed the mode node locations, and therefore the accelerometer and the HSC edge detection locations as being suitable. The impact location is far enough away from the nodal lines to excite all three bending modes. The off centreline impact event would excite all three torsion modes. The aforementioned various locations can be seen in Fig. 4.

Table. 1. Comparison of HI modal test and FEA predicted frequencies.

| Mode | FEA (Hz) | HI (Hz) | Error% |
|------|----------|---------|--------|
| B1   | 35       | 39      | 11     |
| B2   | 103      | 110     | 7      |
| T1   | 183      | 175     | 4      |
| B3   | 210      | 220     | 5      |
| T2   | 560      | 548     | 2      |
| T3   | 961      | 950     | 1      |

### 3.2 HSC visual inspection

Visual inspection has the benefit of using the powerful analysis tools of the human visual system, whereby interpolation and extraction of dynamic events can be achieved with high qualitative capability. The downside is that visual inspection alone cannot extract quantitative results. However, the qualitative evidence from watching the HSC videos of the experimental impact event, allowing user controlled frame replay speeds, shows that T-F phenomenon occurs. It is not possible in this paper to reproduce the dynamic playback images, and a series of static frames does not provide the same visual evidence to the human eye, nor is there enough space in this paper to reproduce enough static images. Instead, a brief text description will be given as an example.

Video playback showed the projectile entered the HSC viewing window and made first contact with the specimen. A displacement wave propagated out from the contact area towards the free end and the clamped end of the specimen. The projectile lost contact with the specimen, which included rotation of the projectile, as a result of a 3° contact angle. During this time the first bending modes appeared. Then higher bending modes became evident and torsion modes, which were confirmed by both the mode shape being visible but also the faster motion as expected due to their higher frequencies. The torsion modes come and go whilst the bending modes continued to be evident. It is not possible to resolve exactly which torsion modes or which bending modes, but it is easy to differentiate between bending and torsion, and have some differentiation between low and higher bending modes. This general behaviour matched the requirements of the strong non-linear definition of T-F behaviour.

### 3.3 STFT criteria

An example simulated signal is shown in Fig. 5, with STFT results for 5ms and 1ms windows shown in

## AMM014

Figs. 6 & 7. The simulated signal S3 is the addition of two signals S1 (220Hz) and S2 (1KHz). S2 is switched off during 6-7ms time record. Fig. 6a and b, 1ms window, shows varying energy content for both S1 and S2 over the full time sample from 0-20ms, but also a significant drop in signal energy at the correct time, highlighted by the black square data point in Fig. 6b. Fig 7, 5ms window, results show only a significant drop in the correct frequency signal over the correct time duration, but not reaching zero energy level. Therefore the key criteria used to determine when a mode had lost all or enough of its energy to be classified as having disappeared required the 1ms window results to drop below or close to zero, and the 5ms results to show a drop over the same time period.

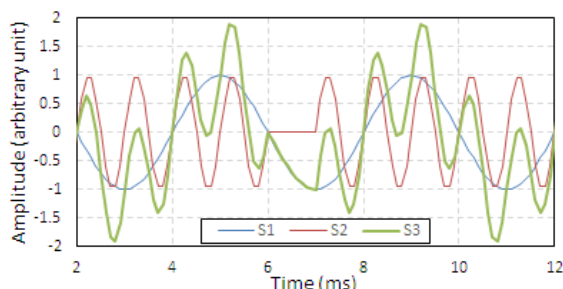


Fig. 5. Arbitrary amplitude time record of the simulated signal used to investigate a choice of criteria for STFT analysis.

### 3.4 T-F comparison between HSC edge detection and FEA results

Figs. 8 and 9 show the STFT analysis examples for B3, T2 and T3, of both the HSC edge detection data for pixel location 950 and the FE simulation data from the same location. Using the established STFT criteria, Fig. 8 shows strong changes to the frequency content over time including dropping down to near zero energy content. In contrast, Fig. 9 FE results show near constant energy content for the modes in the 5ms window analysis. Note that the 1ms window analysis always shows fluctuating amplitude, but this does not mean the actual signal is fluctuating, as shown in the STFT criteria analysis section 3.3. This confirms strong T-F behaviour in the experiments, but not shown in the FE simulation.

## 4. Conclusions

Modal test data validated a linear elastic FE model of a pin-jointed thin flat aluminium plate, impacted by a free flying projectile with its response measured by high speed camera and accelerometers. An STFT analysis shows strongly non-linear behaviour from experimental evidence, but not matched by the FE model. The strongly nonlinear response can be characterised as the modal content forming after the projectile has lost contact, different modes forming at different times, and modes gaining and losing energy more than once and at different times to each other.

Future work includes expanding the experimental test conditions to study effects of key parameters,

improved T-F signal analysis tools, improved instrumentation resolution, development of non-linear models.

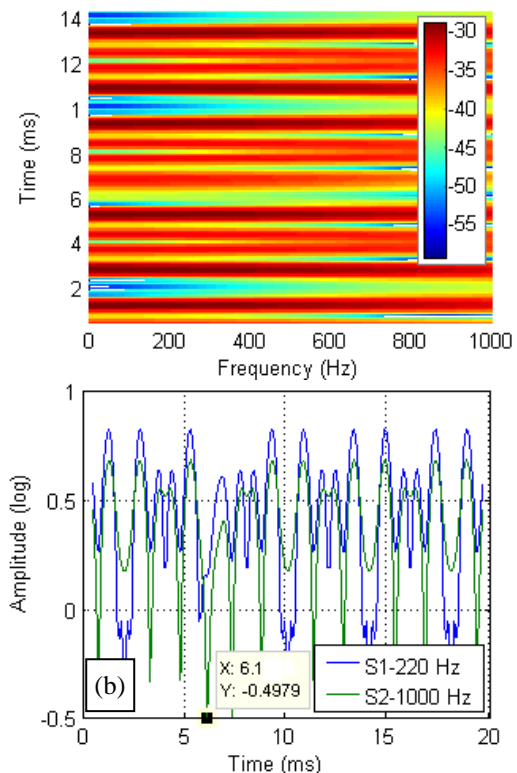


Fig. 6. Simulated signal S3 analysed by STFT 1ms window (a) spectrograph, and (b) log amplitude-time.

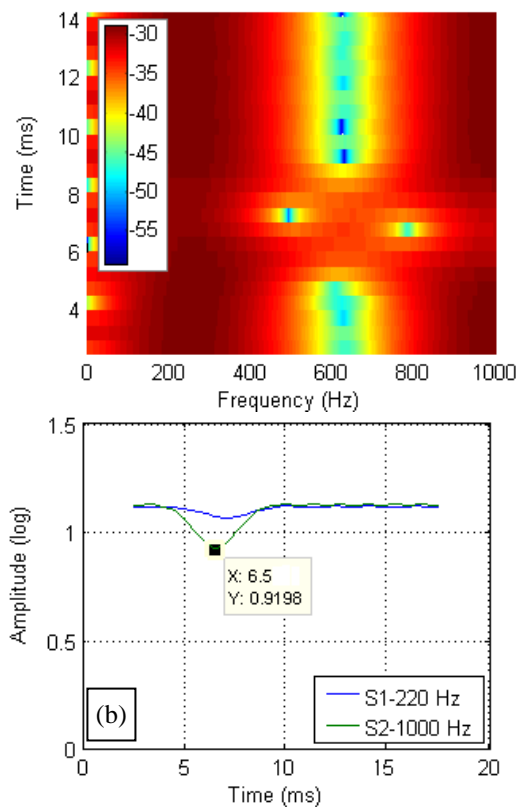


Fig. 7. Simulated signal analysed by STFT 5ms window (a) spectrograph, and (b) log amplitude-time.

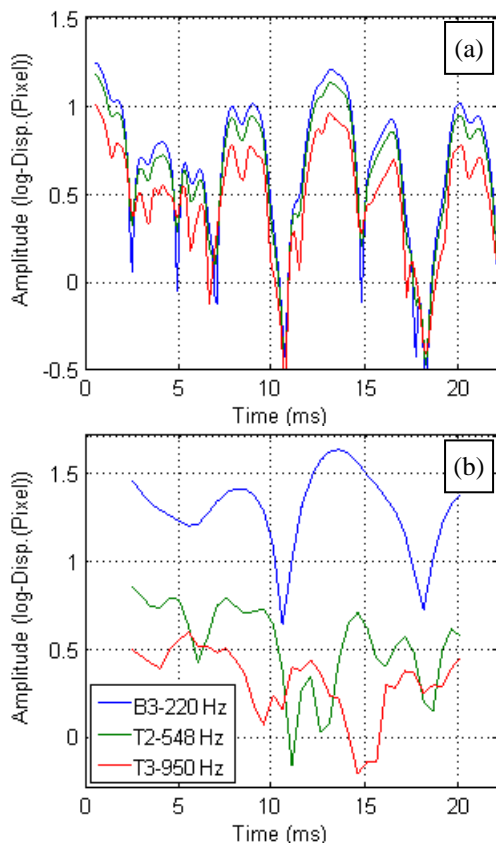


Fig. 8. STFT of HSC edge detection pixel location 950 for B3, T2 & T3, (a) 1ms and (b) 5ms windows.

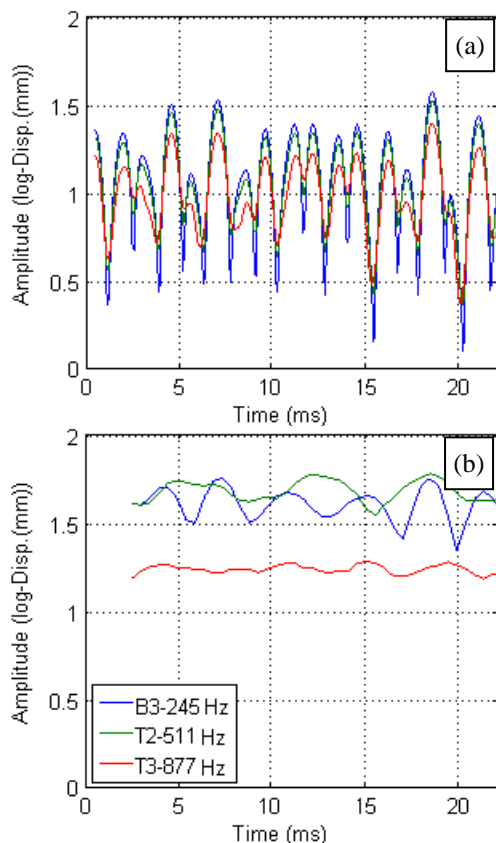


Fig. 9. STFT of FE data, same location and modes as for Fig.8, (a) 1ms and (b) 5ms windows.

## 5. Acknowledgement

The authors are grateful to the National Research Council of Thailand for funding this research. The presenting author is to the U.K. Institution of Mechanical Engineers (IMEchE) for funding his attendance and formal representation of the IMechE at the conference.

## 6. References

- [1] Nagarajaiah S, Basu B, Yang Y, Output only modal identification and structural damage detection using time frequency and wavelet techniques for assessing and monitoring civil infrastructures, Chapter 4 in Sensor Technologies for Civil Infrastructures, (2014) Elsevier, USA.
- [2] Gopalakrishnan S, Mitra M, Wavelet methods for dynamical problems with application to metallic, composite, and nano-composite structures, (2010) CRC Press, USA.
- [3] Xu X, Shi ZY, You Q, Identification of linear time-varying systems using a wavelet-based state-space method, Mechanical Systems and Signal Processing 26 (2012) 91-103.
- [4] Kougioumtzoglou IA, Spanos PD, An identification approach for linear and nonlinear time-variant structural systems via harmonic wavelets, Mechanical Systems and Signal Processing 37 (2013) 338-353.
- [5] Ding Y, Zhao BY, Wu B, Xu GS, Lin Q, Jiang HB, Miao QS, A condition assessment method for time-variant structures with incomplete measurements, Mechanical Systems and Signal Processing 58-59 (2015) 228-244.
- [6] Politopoulos I, Piteau Ph, Antunes J, Borsoi L, Applications of hybrid time-frequency methods in nonlinear structural dynamics, Engineering Structures 68 (2014) 134-143.
- [7] Zucca S, Firrone CM, Nonlinear dynamics of mechanical systems with friction contacts: coupled static and dynamic multi-harmonic balance method and multiple solutions, Journal of Sound and Vibration 333 (2014) 916-926.
- [8] Pai PF, Time-frequency analysis for parametric and non-parametric identification of nonlinear dynamical systems, Mechanical Systems and Signal Processing 36 (2013) 332-353.
- [9] Brake MR, The effect of the contact model on the impact-vibration response of continuous and discrete systems, Journal of Sound and Vibration 332 (2013) 3849-3878.
- [10] Bland, P.W. (2000). Impact Response and Performance of Carbon-Fibre Reinforced Polymers, PhD Thesis, Imperial College. University of London.